ACS APPLIED MATERIALS & INTERFACES

Research Article

www.acsami.org

Sensitive Pb^{2+} Probe Based on the Fluorescence Quenching by Graphene Oxide and Enhancement of the Leaching of Gold Nanoparticles

Xinhao Shi, Wei Gu, Weidong Peng, Bingyu Li, Ningning Chen, Kai Zhao, and Yuezhong Xian*

Department of Chemistry, East China Normal University, Shanghai 200062, People's Republic of China

ABSTRACT: A novel strategy was developed for fluorescent detection of Pb^{2+} in aqueous solution based on the fact that graphene oxide (GO) could quench the fluorescence of amino pyrene (AP)-grafted gold nanoparticles (AP–AuNPs) and Pb^{2+} could accelerate the leaching rate of AuNPs in the presence of $S_2O_3^{2-}$. In this system, fluorescence reporter AP was grafted on AuNPs through the Au–N bond. In the presence of GO, the system shows fluorescence quenching because of $\pi-\pi$ stacking between AP and GO. With the addition of Pb^{2+} and $S_2O_3^{2-}$, the system displays fluorescence recovery, which is attributed to the fact that Pb^{2+} could accelerate the leaching of the AuNPs from GO surfaces and release of AP into aqueous solution. Interestingly, the concentration of GO could control the fluorescence "turn-off" or "turn-on" for Pb^{2+} detection. In addition, GO is also an excellent promoter for the acceleration of the leaching of AuNPs and shortening the analytical time to ~15 min. Under the optimal conditions, the fluorescence Pb^{2+} sensor shows a linear range from 2.0×10^{-9} to 2.3×10^{-7} mol/L, with a detection limit of 1.0×10^{-10} mol/L.

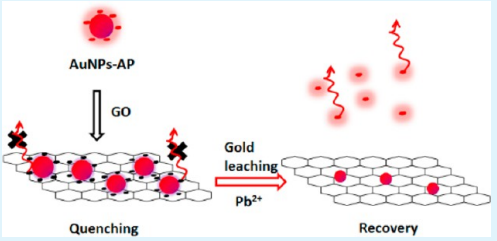

KEYWORDS: *graphene oxide, gold nanoparticles, amino pyrene, Pb^{2+}, fluorescence sensor*

INTRODUCTION

Graphene oxide (GO), as a specific branch of graphene, has a two-dimensional, atomically thin nanostructure with a range of reactive oxygen functional groups, such as carboxylic acid, phenol hydroxyl, and epoxide groups.[1] In contrast to ideal graphene with 100% sp^2-hybridized carbon atoms, GO is comprised of sp^2/sp^3 structure.[2] The unique structure leads to the most notable difference between GO and graphene, which is the optoelectronic properties because of the finite bandgap in GO.[3,4] GO shows intrinsic and tunable fluorescence in the region of red/near-infrared, visible, and ultraviolet light[4−6] and offers exciting opportunities in nanomedicine and chemo-/biosensing.[7−9] Besides itself fluorescence, GO is also an excellent quencher for fluorescent moieties. On the basis of the fluorescence quenching properties of GO, various optical sensors have been developed for the detection of biomolecules, metal ions, etc. As for the biomolecule measurement, for example, Lu and colleagues demonstrated the utility of water-soluble GO for sensitive and selective detection of DNA and human thrombin because GO could quench the fluorescence of dye-labeled ssDNA or aptamer.[10] On the basis of the findings that GO possesses high fluorescence quenching ability as well as different affinities toward ss- and dsDNA, He and co-workers designed a multicolor sensor for homogeneous, multiplex, sequence-specific DNA detection.[11] Wang and co-workers reported a proof of principle of the intracellular protease sensor using GO as the nanocarrier for the peptide and quencher for fluorophores.[12] Very recently, a sensitive and selective miRNA assay was developed by coupling the fluorescence quenching of GO with site-specific cleavage of an endonuclease.[13] In addition, a biosensing platform for the detection of protein kinase activity based on the GO–peptide nanocomplex and phosphorylation-induced suppression of carboxypeptidase Y cleavage was also reported.[14] Owing to the tunable fluorescence properties of silver nanoclusters, Liu et al. demonstrated the multiplexed analysis of DNAs of infectious pathogens using a hybrid system consisting of nucleic-acid-functionalized silver nanoclusters and GO.[15] Some other biomolecules, such as dopamine,[9] hemin,[16] metalloproteinase,[17] heparin,[18] etc., were also measured by a GO-based fluorescent biosensor.

Owing to the increasing threat of heavy metal contaminations in the environment and the severe effects on human health, developing a versatile strategy for trace detection of heavy metal ions in aquatic ecosystems is of great interest. In the past few years, GO-based fluorescence nanoprobes for heavy metal ion detection have been reported. A fluorescent GO/poly(vinyl alcohol) hybrid was synthesized and used as a "turn-off" probe for Au^{3+} ions in aqueous media, which was based on the fact that Au^{3+} could quench the fluorescence of the hybrid.[19] Butylamine-modified GO was used to build a logic gate for the discrimination of Fe^{3+} and Fe^{2+} in living cells because the fluorescence of GO could be strongly quenched by Fe^{3+} or in the presence of Fe^{2+} and H_2O_2.[20] Wang and co-workers presented a method to tailor the lateral size of GO in the range of 10–100 nm, and the nanosheets could be used as a fluorescent probe to detect Fe^{3+} ions.[21] However, these "turn-off" sensing strategies are not suitable for real sample measurements because false signals might be obtained as a

Received: November 8, 2013
Accepted: January 29, 2014
Published: January 29, 2014

   dx.doi.org/10.1021/am405012k | ACS Appl. Mater. Interfaces 2014, 6, 2568−2575

Scheme 1. Schematic Illustration of Fluorescence Sensing of Pb^{2+} Based on Fluorescence Quenching of GO and Enhancement of the Leaching of AuNPs

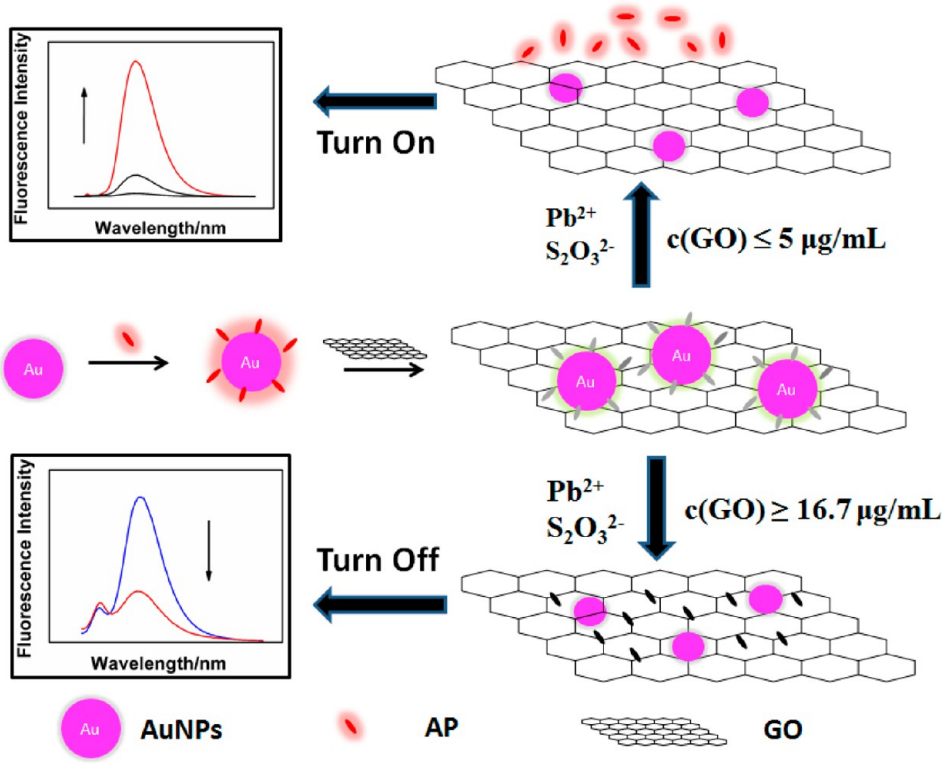

result of the presence of unexpected quenching entities. Recently, a functional nucleic acid–GO hybrid system was developed for "turn-on" fluorescent detection of heavy metal ions. In the sensing system, functional nucleic acid was used as a recognition unit and GO was used as a fluorescence quencher. On the basis of this strategy, various metal ions, such as Ag^{+},[22,23] Fe^{2+},[24] Cu^{2+},[25] Pb^{2+},[26] Hg^{2+},[27,28] etc., were detected successfully. In addition, metal-ion-dependent DNAzymes were also introduced into a GO-based system for heavy metal ion detection.[29−31] However, many of these systems have limited practical application because of the high cost, complicated processing, and ease to denature.

In this work, we propose a "turn-on" fluorescent sensing strategy for rapid, ultrasensitive, and cost-effective detection of Pb^{2+} in aqueous solution (Scheme 1). Amino pyrene (AP) is used as a fluorescent reporter and grafted on gold nanoparticles (AuNPs) through the Au–N bond. GO acts as a fluorescent quencher for AP because of $\pi-\pi$ stacking between AP and GO. On the basis of the fact that Pb^{2+} could accelerate the leaching rate of the AuNPs in the presence of thiosulfate and the fluorescence could be recovered, a simple "mix-and-detect" type of fluorescence sensor is developed for Pb^{2+} measurement with high sensitivity and selectivity. Very interestingly, the concentration of GO could control the fluorescence "turn-off" or "turn-on" for Pb^{2+} detection. Moreover, GO is also an excellent promoter for the acceleration of the leaching of AuNPs, and the analytical time can be shortened obviously.

EXPERIMENTAL SECTION

Reagents. AP was purchased from Sigma-Aldrich. Gold chloride trihydrate, $PbCl_2$, ethanol, and the other common reagents were purchased from Sinopharm Chemical Reagent (Shanghai, China).

Synthesis of GO. GO was synthesized according to a modified Hummers method.[32] In a typical experiment, 1.0 g of graphite powder was first dispersed in concentrated, 23 mL of H_2SO_4 and stirred for 12 h at room temperature. Then, 3 g of $KMnO_4$ was slowly added to the mixture under vigorous stirring at 0 °C. The mixture was sonicated for 10 h to give a dark-green solution. Then, 46 mL of ultrapure water was gradually transferred to the reaction system. After the mixture was kept boiling for 20 min, the reaction was terminated by the addition of 140 mL of ultrapure water and 10 mL of H_2O_2 (30%). Finally, the product was separated by centrifugation and then washed with 5% HCl and ultrapure water 3 times.

Synthesis of AuNPs. AuNPs were synthesized with a method as reported by Birrell et al.,[33] with minor modifications. Aliquots (10 μL) of freshly prepared $NaBH_4$ (0.1 mol/L) were added slowly into $HAuCl_4$ (0.25 mM, 8 mL) at 22 °C until a stable purple-colored colloid was observed, and then the reaction was left for 24 h at 22 °C. The concentration of the AuNPs was calculated according to Beer's law as 2.3 nM.

Quenching of AP–AuNPs by GO Sheets. The quenching procedure was conducted through grafting AP onto AuNPs (AP–AuNPs) and a simple mixing of AP–AuNPs with GO sheets (GO/AP–AuNPs). Typically, 30 μL of AP (10^{-5} M) aqueous solution was added to 3 mL of 2.3 nM AuNPs solution. After incubation for 6 h, different concentrations of GO were dropped into the AP–AuNPs solution to investigate the fluorescence response.

Fluorescence Detection. The fluorescence recovery was realized through gold leaching. Typically, 10 μL of $Na_2S_2O_3$ was added to 3 mL of the GO/AP–AuNPs aqueous solution, and then different concentrations of Pb^{2+} were added and incubated at room temperature for 15 min. After that, the fluorescence was measured.

Instruments. A Fourier transform infrared (FTIR) spectrum was recorded on a NEXLIS FTIR (Nicolet, U.S.A.) spectrometer, and samples were dried at 90 °C in vacuum for 3 h prior to fabrication of the KBr pellet. An atomic force microscopy (AFM) image was recorded in air using a Digital Instruments Nano Scope IIIa. The Raman spectrum was obtained by a confocal Raman 35 microscope (CRM200, WITec). Ultraviolet–visible (UV–vis) absorption spectra

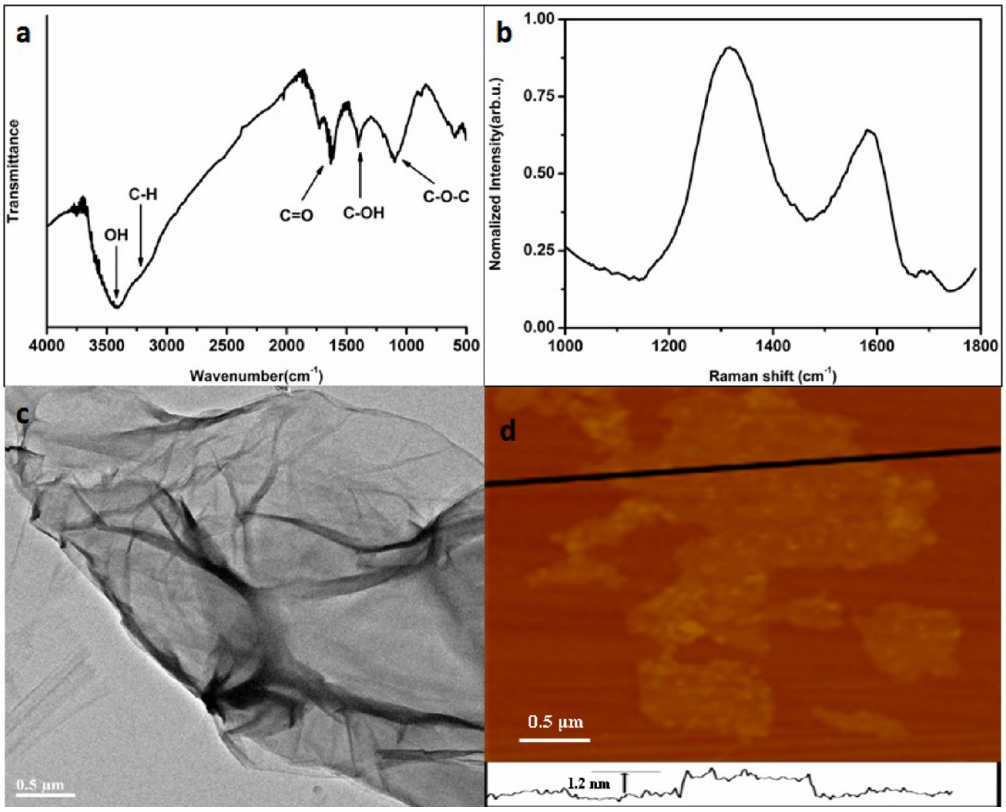

Figure 1. (a) FTIR, (b) Raman, (c) TEM, and (d) AFM characterizations of GO.

were recorded on a Shimadzu UV-2550 spectrophotometer (Shimadzu, Japan). The fluorescence spectra were obtained on a Hitachi F-7000 fluorescence spectrometer (Hitachi, Japan). The transmission electron microscopy (TEM) images were performed on a JEM-2100F transmission electron microscope (JEM, Japan).

RESULTS AND DISCUSSION

Characterization of GO. As shown in Figure 1a, the FTIR spectrum shows that GO has typical oxygen-containing groups, such as O−H (3420 cm^{-1}), C═O (~1700 cm^{-1}), C−OH (1310 cm^{-1}), and C−O−C (1200 cm^{-1}). The Raman spectrum (Figure 1b) demonstrates a typical D band (~1320 cm^{-1}) and G band (~1570 cm^{-1}) for GO. The intensity ratio (I_D/I_G) is characteristic of the extent of disorder of carbon networks within in the material.[34] In this case, the I_D/I_G of 1.43 indicates the high occupation of oxygen-rich groups and defects. Moreover, as shown in the TEM image (Figure 1c), the characteristic transparent and paper-like morphology of GO is observed. In addition, the height of the GO sheet is about 1.2 nm based on the cross-sectional view of the typical AFM image (Figure 1d).

Quenching AP−AuNPs with GO. Figure 2a shows the TEM image of the as-prepared AuNPs. The AuNPs are generally spherical, and the particle sizes are ~10 nm. The GO sheets display the characteristic paper-like morphology, and AP−AuNPs are homogeneously decorated on the plane of GO in the composite of GO/AP−AuNPs, as shown in Figure 2b. In addition, it can be seen that, at the edge of GO sheets, the AuNPs agglomerate to some extent because of the higher surface energy and more hydrophilic oxygen-containing groups.[35]

Figure 3 exhibits the UV−vis absorption spectra of AP, GO, AP−AuNPs, and GO/AP−AuNPs. As shown in Figure 3, in the

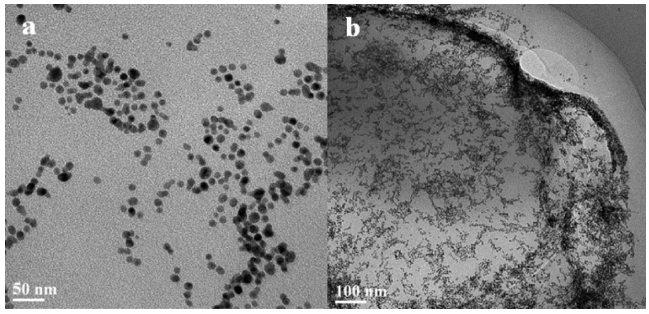

Figure 2. TEM images of (a) AuNPs and (b) GO/AP−AuNPs.

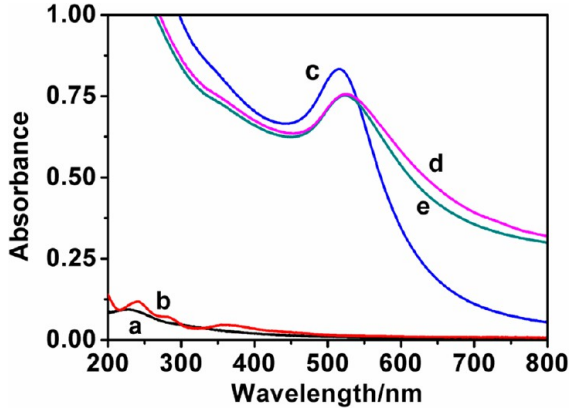

Figure 3. UV adsorption spectra of (a) GO (5 μg/mL), (b) AP (1 μM), (c) AuNPs (2.3 nM), (d) AP−AuNPs (2.3 nM), and (e) GO/AP−AuNPs.

dx.doi.org/10.1021/am405012k | ACS Appl. Mater. Interfaces 2014, 6, 2568−2575

near-UV region, weak absorption is observed for AP (1 μM) (Figure 3a) and GO (5 μg/mL) (Figure 3b). As for AuNPs colloid (Figure 3c), the maximum absorption at 515 nm can be attributed to the surface plasmon resonance (SPR) of AuNPs. Associated with the TEM image, the concentration of the AuNPs is calculated as 2.3 nM according to Beer's law using an extinction coefficient of 3.7×10^8 for the ~10 nm AuNPs.[36] With the addition of AP, the SPR of AuNPs is damped (Figure 3d), indicating the attachment of AP molecules on AuNPs. It is well-known that gold atoms on the surface of the nanoparticles possess unoccupied orbitals for nucleophiles to donate electrons;[37] thus, strong electron donors, for example, AP, could donate electrons to the vacant orbitals on the gold surface to form AP−AuNPs. After continuous addition of GO, the absorption is almost the same as that of AP−AuNPs (Figure 3e), indicating that the interaction between GO and AP−AuNPs is through physical adsorption.

Enhancement of Gold Leaching. It was reported that Pb^{2+} could accelerate the leaching of AuNPs in the ammonia−thiosulfate system.[38] On the basis of this principle, colorimetric detection of Pb^{2+} was developed by Huang and co-workers[39,40] and Wu and co-workers[41] through measurement of the changes in the SPR of the AuNPs. To understand the roles of $S_2O_3^{2-}$ and Pb^{2+} for gold leaching in the GO/AP−AuNPs system, the SPR of the AuNPs was recorded. Figure 4a shows the UV

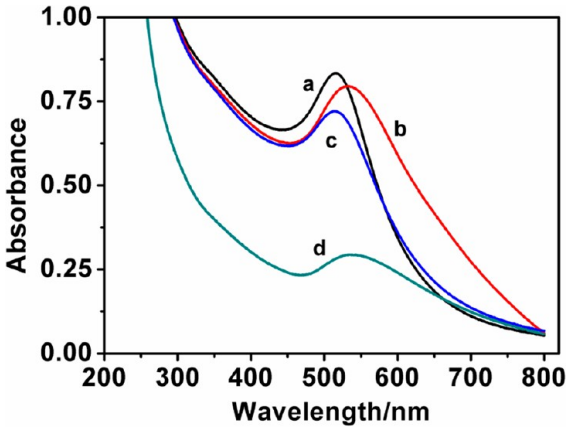

Figure 4. UV−vis absorption spectra of (a) GO/AP−AuNPs, (b) GO/AP−AuNPs + $S_2O_3^{2-}$, (c) GO/AP−AuNPs + Pb^{2+}, and (d) GO/AP−AuNPs + $S_2O_3^{2-}$ + Pb^{2+}. The concentrations of $Na_2S_2O_3$ and $PbCl_2$ were 0.1 mM and 0.1 μM, respectively.

spectrum of GO/AP−AuNPs. After the addition of 1 mM $S_2O_3^{2-}$, the adsorption intensity decreases slightly and a red shift of the maximum absorption is observed (Figure 4b). It is because the $S_2O_3^{2-}$ ions could react with gold atoms in the presence of O_2 to generate $Au(S_2O_3^{2-})_2^{3-}$ complexes (as described in reaction 1), owing to the low spin d^{10} Au^+ ions.[42]

$$4Au^0 + O_2 + 2H_2O + 8S_2SO_3^{2-} \rightarrow 4Au(S_2SO_3)_2^{3-} + 4OH^- \quad (1)$$

The addition of Pb^{2+} in the GO/AP−AuNPs system also leads to the decrease in intensity and a slight red shift of the absorbance peak (Figure 4c). It might be ascribed to the fact that Pb^{2+} could react with a gold atom to form $AuPb_2$, $AuPb_3$ alloy, or metallic Pb on the surface of AuNPs,[43,44] which results in a slight aggregation of AuNPs and causes the decrease and red shift of absorbance.[45] Figure 4d shows the SPR of GO/AP−AuNPs in the presence of $S_2O_3^{2-}$ and Pb^{2+} simultaneously. It can be seen that the SPR of AuNPs is reduced dramatically, indicating a large degree of gold dissolution, owing to the Pb^{II}-catalyzed leaching of AuNPs in the $S_2O_3^{2-}$ system. It is also confirmed by the TEM image in Figure 5; only a few AuNPs can be observed on the GO surface after leaching by Pb^{2+}.

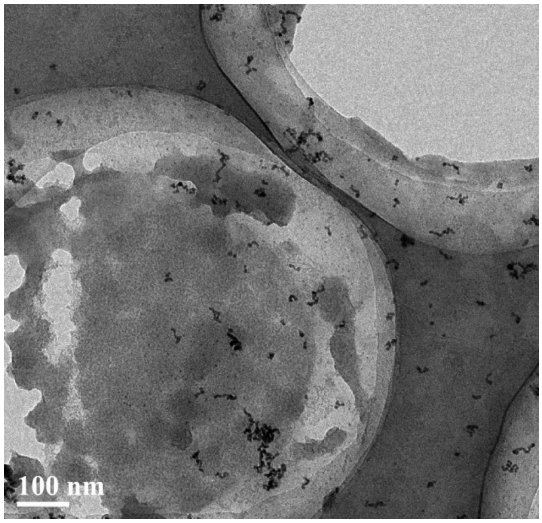

Figure 5. TEM image of GO/AP−AuNPs with 1 mM $S_2O_3^{2-}$ and 0.1 μM Pb^{2+}.

Effect of GO on Gold Leaching. As shown in reaction 1, $S_2O_3^{2-}$ could dissolve gold into the bulk solution in forms of $Au(S_2O_3^{2-})_2^{3-}$ complexes, with oxygen gas as an oxidant. However, the leaching rate of AuNPs is very slow because of a high activation energy (E_a = 27.99 kJ/mol).[46] In the presence of metal mediators, for example, Pb^{2+} could accelerate the leaching rate of gold by reducing the active energy.[38] Nevertheless, the leaching rate of AuNPs is still slow in the presence of $S_2O_3^{2-}$ and Pb^{2+}. To further enhance the leaching rate of gold, Huang et al.[39] found that the addition of 2-mercaptoethanol (2-ME) could form $Au(2\text{-ME})_2$ complexes and accelerate the leaching of AuNPs in the ammonia−thiosulfate system. On the basis of this finding, a colorimetric assay for Pb^{2+} is developed in the 2-ME/$S_2O_3^{2-}$−AuNPs system. However, the leaching process is still time-consuming, and 2 h is need. In addition, 2-ME is considered toxic and easy to be oxidized in an air atmosphere. Chen and co-workers[47] reported "turn-on" fluorescence detection of Pb^{2+} based on the fact that Pb^{2+} could accelerate the leaching rate of the AuNPs on graphene surfaces in the presence of $S_2O_3^{2-}$ and 2-ME; however, the analytical time is over 1 h. In addition, toxic 2-ME is also used. Recently, Wu and co-workers reported that hexadecyl trimethyl ammonium bromide, as a stabilizing agent for AuNPs, could accelerate the adsorption of $S_2O_3^{2-}$ on the surface of the AuNPs and enhance the leaching of gold within 30 min.[41]

In our system, we found that GO could accelerate gold leaching in the GO/AuNPs system in the presence of $S_2O_3^{2-}$ and Pb^{2+} within 15 min. Figure 6 shows the SPR of AuNPs with the reaction time in the presence and absence of GO. In both situations, the absorption of AuNPs decreases with the increase of the reaction time because of the leaching of AuNPs by Pb^{2+}. However, in the absence of GO (Figure 6a), the SPR decreases with time up to ~40 min and then levels off in the presence of 1 mM $S_2O_3^{2-}$ and 100 nM Pb^{2+}. In contrast, in the presence of

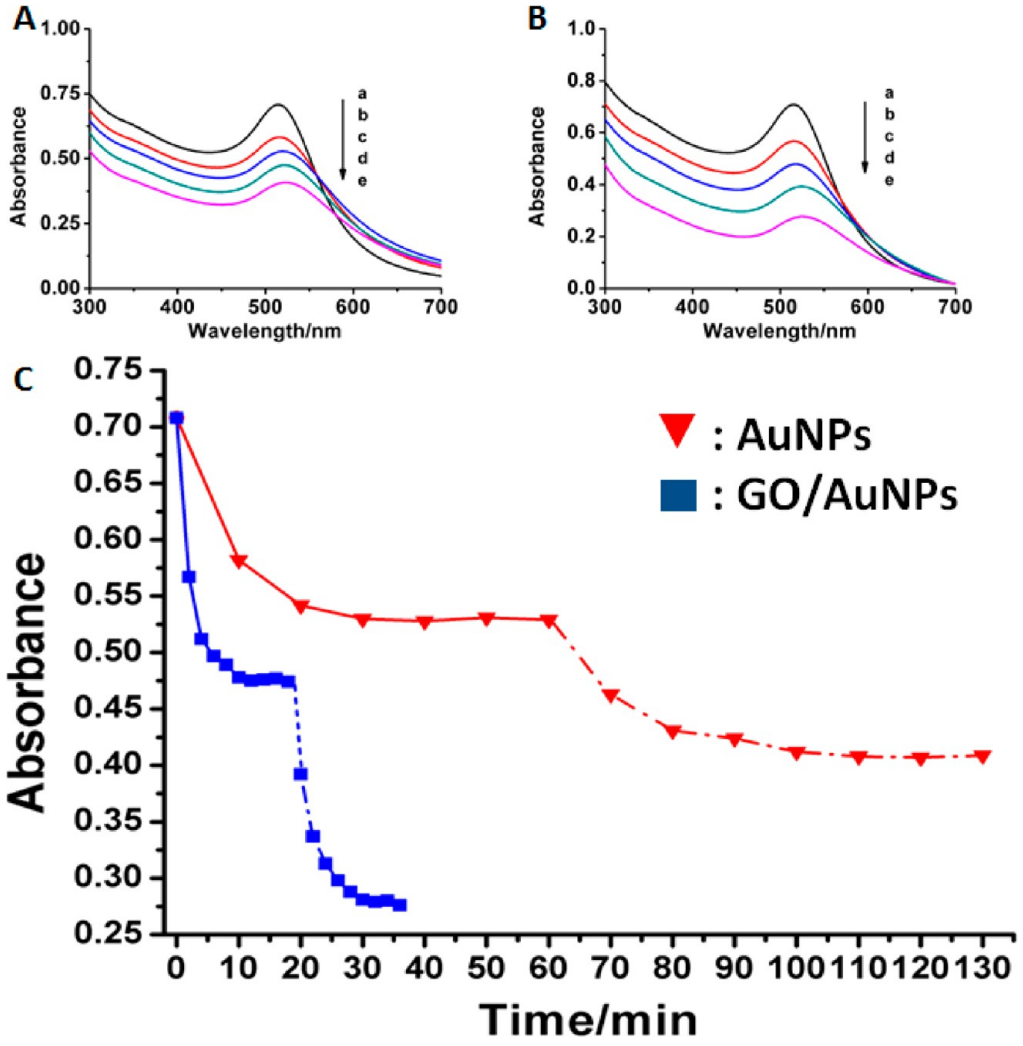

Figure 6. (A) UV−vis spectra of AP−AuNPs (2.3 nM) with the addition of $S_2O_3^{2-}$ for (a) 0 min, (b) 5 min (c) 50 min, and then consecutive addition of Pb^{2+} for (d) 5 min and (e) 50 min. (B) UV−vis spectra of GO/AP−AuNPs after the addition of $S_2O_3^{2-}$ for (a) 0 min, (b) 3 min, (c) 18 min, and then consecutive addition of Pb^{2+} for (d) 3 min and (e) 15 min. (C) Plots of SPR versus reaction time for AuNPs and the GO/AP−AuNPs system, respectively (solid line, addition of $S_2O_3^{2-}$; dash line, addition of Pb^{2+}).

GO (Figure 6b), the leaching process reaches equilibrium within 15 min. It shows that GO plays a very important role for gold leaching.

Given the structure and properties of GO, it is supposed that GO could enrich $S_2O_3^{2-}$ and Pb^{2+}, which equivalently increases the concentration of reactants and induces stronger etching. For AuNPs, graphene and its derivatives show well physisorption for gold nanoparticles, while no significant chemical interaction is expected.[48,49] The TEM images of Figure 2 confirm the combination of GO and AuNPs. On the other hand, besides the physical adsorption, metal ions could strongly bond to GO through metal−carbonyl coordination.[50] Overall, the enrichment of AuNPs and lead ions equivalently enhances the concentration of reactants and facilitates the gold leaching.

Fluorescence Sensing. To verify the sensing strategy, the fluorescence spectra of AuNPs, GO, and AP were monitored first. As shown in Figure 7, AuNPs (Figure 7f) and GO (Figure 7e) display ignorable fluorescence emission. As for AP (Figure 7b), a strong fluorescence emission at 440 nm is observed, which corresponds to the monomeric form of fluorophore in water. After grafted on AuNPs, the fluorescence intensity of AP

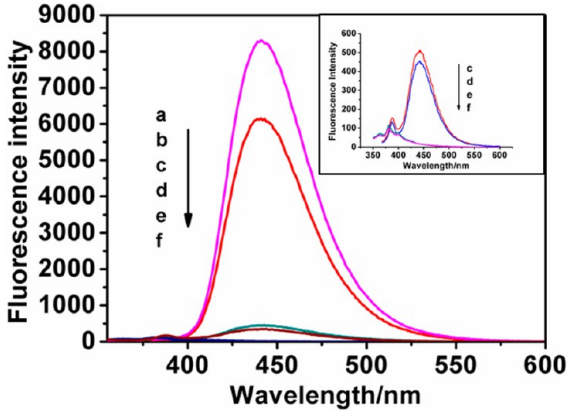

Figure 7. Fluorescence spectra of (a) AP−AuNPs, (b) AP (0.1 μM), (c) GO/AP−AuNPs + $Na_2S_2O_3$ (1 mM), (d) GO/AP−AuNPs, (e) GO (5 μg/mL), and (f) AuNPs (2.3 nM). (Inset) Amplification of spectra of c−f. λ_{ex}, 340 nm; slit width, 5 × 5 nm.

increased (Figure 7d) because of the proximity effects. AP was grafted on AuNPs through the Au−N interaction and donated electrons from a particular distance to the gold surface, which

dx.doi.org/10.1021/am405012k | ACS Appl. Mater. Interfaces 2014, 6, 2568−2575

dominated the luminescence properties of the fluorophores by the highly localized near-field interactions and led to fluorescence enhancement of the probe molecules.[51] With the addition of GO, the fluorescence intensity is dramatically decreased (Figure 7d). In this work, with 2.3 nM AP−AuNPs mixing with 5 μg/mL GO, the fluorescence intensity is reduced from 8200 to 510, with a very high quenching efficiency of 93.62%. After the addition of 1 mM $S_2O_3^{2-}$, the AuNPs could not be leached and, thereby, the fluorescence is still low (Figure 7c). However, after the addition of Pb^{2+}, AuNPs are leached and the fluorescence intensity shows a dramatic change.

Effect of the GO Concentration on Fluorescence Sensing. As mentioned above, GO can accelerate the leaching of AuNPs. In addition, GO is also a fluorescent quencher. Thus, the concentration of GO might affect the fluorescence response of AP−AuNPs. Various amounts of GO (3.3, 5.0, 8.3, 12.5, and 16.7 μg/mL) were added in AP−AuNPs colloids in the presence of 1 mM $S_2O_3^{2-}$ and 100 nM Pb^{2+}. We find that the fluorescence response of the sensing system to Pb^{2+} is strongly dependent upon the relative amount of GO. The concentration of GO could control the fluorescence switch "on" or "off" for Pb^{2+} detection. As a result, the system shows an optical "turn-on" phenomenon because the concentration of GO is less than or equal to 5 μg/mL. In contrast, when the concentration of GO is ≥16.7 μg/mL, the system exhibits a typical "turn-off" condition. Figure 8 displays the fluorescence spectrum of AP−AuNPs in the presence of 16.7 μg/mL GO, and a fluorescence emission at 440 nm for AP is observed. With the increase of the concentration of Pb^{2+}, the fluorescence intensity decreases. This "turn-off" switch indicates that, at higher concentrations, the probe molecular AP could be adsorbed onto GO sheets again after gold leaching.

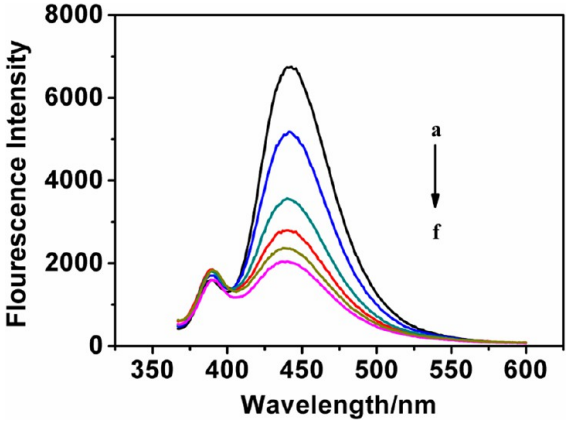

Figure 8. Fluorescence spectra of 2.3 nM AP−AuNPs in 16.7 μg/mL GO solution upon the addition of 1 mM $S_2O_3^{2-}$ and different concentrations of Pb^{2+} (a−f, addition of 0.2 μM each). λ_{ex}, 340 nm; slit width, 10 × 10 nm.

The "turn-on" and "turn-off" models modulated by the concentration of GO could be explained by the competition between adsorption and diffusion of the detached AP molecule from AuNPs. As shown in Scheme 2, at higher concentrations ([GO] ≥ 16.7 μg/mL), the adsorption of AP by GO occupies the domination and leads to fluorescence "turn-off". At lower concentrations ([GO] ≤ 5 μg/mL), the diffusion of AP is dominant and results in fluorescence "turn-on". However, higher concentrations of GO greatly affect the detection sensitivity toward Pb^{2+} because of scattering.

Scheme 2. Schematic Illustration of the Fluorescent Switch Modulated by the Concentration of GO

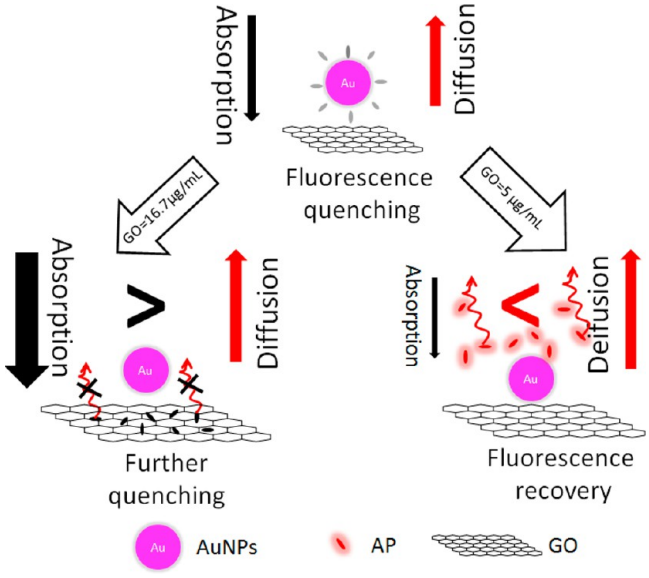

Thus, the "turn-on" model was chosen for further study. Under the "turn-on" model, the system containing 5 μg/mL GO, 2.3 nM AP−AuNPs, and 1 mM $Na_2S_2O_3$ was used for Pb^{2+} detection. As shown in Figure 9, the fluorescence intensity increases upon the addition of Pb^{2+} and shows a well linear response over the range from 2 to 233 nM with a correlation coefficient (R^2) of 0.99588 (as shown in the inset of Figure 9). The limit of detection (LOD; S/N = 3) for Pb^{2+} ions is as low as 0.1 nM.

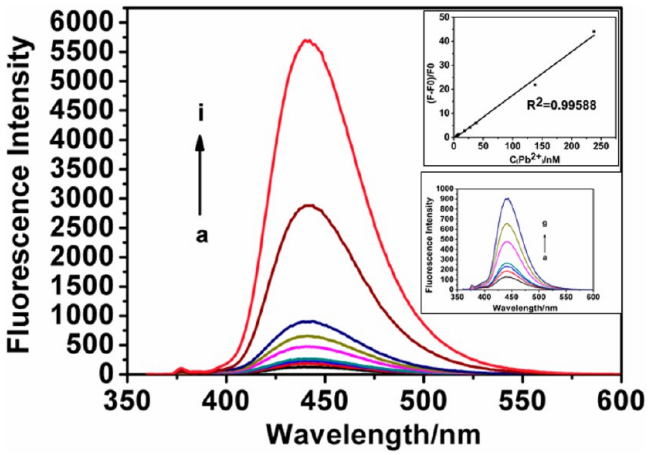

Figure 9. Fluorescence spectra of 5 μg/mL GO and 2.3 nM AP−AuNPs in 1 mM $Na_2S_2O_3$ with the addition of Pb^{2+} ions [the concentrations of Pb^{2+} ions in solution were (a) 0 nM, (b) 1 nM, (c) 2 nM, (d) 3 nM, (e) 13 nM, (f) 23 nM, (g) 33 nM, (h) 133 nM, and (i) 233 nM]. The top inset is the calibration curve for Pb^{2+} detection, and the bottom inset is the amplified fluorescence spectra of a−g.

To further evaluate the selectivity of this "turn-on" fluorescence sensor for Pb^{2+}, various metal ions, such as Cd^{2+}, Mg^{2+}, Zn^{2+}, Hg^{2+}, Co^{2+}, Cu^{2+}, Ag^{+}, Fe^{3+}, and Mn^{2+}, were added in the system and the fluorescence responses were measured. As shown in Figure 10, this system shows excellent selectivity toward Pb^{2+} by a factor of 100-fold or more relative to the other metal ions. It should be noted that Hg^{2+} is a

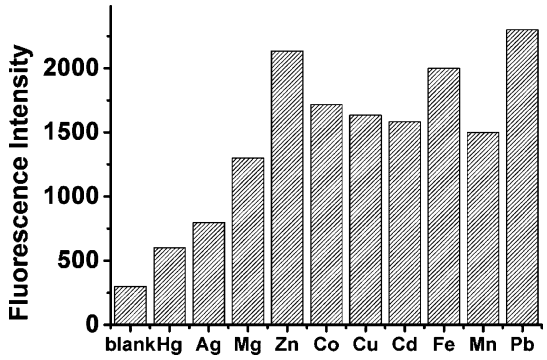

Figure 10. Relative fluorescence responses of GO/AP−AuNPs in 1 mM $Na_2S_2O_3$ upon the addition of various metal ions. The concentration of Cd^{2+}, Mg^{2+}, Zn^{2+}, Hg^{2+}, Co^{2+}, Cu^{2+}, Ag^{+}, Fe^{3+}, and Mn^{2+} was 10 μM, and the concentration of Pb^{2+} was 100 nM.

universal interfering ion in the detection of Pb^{2+}. However, in this work, Hg^{2+} does not results in an obvious fluorescence change even at high concentrations. It suggests that the "turn-on" fluorescence sensor provides a promising alternative to Pb^{2+} determination in the presence of Hg^{2+} without universal masking agents of Hg^{2+}. Therefore, the fluorescence sensor could meet the requirements for practical applications.

Pb^{2+} Detection in Real Samples. To evaluate the practicality of our approach, real samples, such as mineral water, drinking pure water, tap water, and river water, were used for the practical assay (shown in Table 1). No Pb^{2+} was

Table 1. Recoveries for Pb^{2+} Detection in the Real Water Samples (n = 3)

samples	Pb^{2+} (nM) (n = 3)	addition (nM) (n = 3)	found (nM) (n = 3)	recovery (%)	RSD (%)
mineral water	0	5	4.53	90.6	5.04
	0	40	39.28	98.2	1.42
	0	200	216	108	7.30
drinking pure water	0	5	4.65	93	1.54
	0	40	40.96	102.4	2.37
	0	200	210.6	105.3	2.12
tap water (10-fold diluted)	18	5	23.46	109.2	5.83
		40	55.72	94.3	3.46
		100	117.6	99.6	1.72
river water (20-fold diluted)	100	5	105.22	104.3	8.21
		40	142.56	106.4	2.33
		100	205.9	105.9	2.69

detected in the mineral water and drinking pure water samples. Thus, the standard addition method was used for Pb^{2+} measurement. For mineral water samples, the recovery for Pb^{2+} is over the range of 90.6−108% and the relative standard deviation (RSD) is over 1.42−7.3%. As for drinking pure water samples, the recovery is over 93−105.3%, with the RSD of 1.54−2.37%. With regard to tap water and river water samples, Pb^{2+} was successfully detected in the 10-fold diluted tap water and 20-fold river water samples. The concentration of Pb^{2+} is about 180 nM for tap water and 2.0 μM for river water. Furthermore, the standard addition method is also adopted to verify the feasibility of the assay in tap water and river water samples, and the RSD ranged from 1.72 to 8.21%. The results confirm that the GO/AP−AuNPs sensing system has potential application for the Pb^{2+} measurement in drinking and environmental water samples.

CONCLUSION

In summary, this work reported a "turn-on" fluorescence sensor for rapid, sensitive, and selective detection of Pb^{2+}. In this system, GO acts as a super fluorescence quencher as well as an accelerator for gold leaching. In addition, when the advantages of Pb^{2+} enhancement of gold leaching are taken into account, the optical sensor allows for the determination of Pb^{2+} as low as 0.1 nM and shows a linear range from 2 to 233 nM. In addition, the sensing strategy could shorten the analytical time to about 15 min because of the enhancement effect by GO. Moreover, the Pb^{2+} probe exhibits high selectivity over other possible interference ions and satisfactory recoveries for water sample analysis. Therefore, this sensing strategy provides a simple, quick, and sensitive method for the detection of heavy metal ions in water samples.

AUTHOR INFORMATION

Corresponding Author

*Telephone/Fax: 86-21-54340046. E-mail: yzxian@chem.ecnu.edu.cn.

Notes

The authors declare no competing financial interest.

ACKNOWLEDGMENTS

This work was supported by the National Natural Science Foundation of China (21175046) and the Open Foundation of Shanghai Key Laboratory of Green Chemistry and Chemical Process.

REFERENCES

(1) Dreyer, D. R.; Park, S.; Bielawski, C. W.; Ruoff, R. S. *Chem. Soc. Rev.* **2010**, *39*, 228−240.
(2) Cai, W.; Piner, R. D.; Stadermann, F. J.; Park, S.; Shaibat, M. A.; Ishii, Y.; Yang, D.; Velamakanni, A.; An, S. J.; Stoller, M.; An, J.; Chen, D.; Ruoff, R. S. *Science* **2008**, *321*, 1815−1817.
(3) Boukhvalov, D. W.; Katsnelson, M. I. *J. Am. Chem. Soc.* **2008**, *130*, 10697−10701.
(4) Eda, G.; Lin, Y. Y.; Mattevi, C.; Yamaguchi, H.; Chen, H. A.; Chen, I. S.; Chen, C. W.; Chhowalla, M. *Adv. Mater.* **2010**, *22*, 505−509.
(5) Luo, Z.; Vora, P. M.; Mele, E. J.; Johnson, A. T. C.; Kikkawa, J. M. *Appl. Phys. Lett.* **2009**, *94*, 11909.
(6) Loh, K. P.; Bao, Q.; Eda, G.; Chhowalla, M. *Nat. Chem.* **2010**, *2*, 1015−1024.
(7) Sun, X.; Liu, Z.; Welsher, K.; Robinson, J. T.; Goodwin, A.; Zaric, S.; Dai, H. *Nano Res.* **2008**, *1*, 203−212.
(8) Liu, Z.; Robinson, J. T.; Sun, X.; Dai, H. *J. Am. Chem. Soc.* **2008**, *130*, 10876−10877.
(9) Chen, J. L.; Yan, X. P.; Meng, K.; Wang, S. F. *Anal. Chem.* **2011**, *83*, 8787−8793.
(10) Lu, C. H.; Yang, H. H.; Zhu, C. L.; Chen, X.; Chen, G. N. *Angew. Chem., Int. Ed.* **2009**, *48*, 4785−4787.
(11) He, S.; Song, B.; Li, D.; Zhu, C.; Qi, W.; Wen, Y.; Wang, L.; Song, S.; Fang, H.; Fan, C. *Adv. Funct. Mater.* **2010**, *20*, 453−459.
(12) Wang, H.; Zhang, Q.; Chu, X.; Chen, T.; Ge, J.; Yu, R. *Angew. Chem., Int. Ed.* **2011**, *50*, 7065−7069.
(13) Tu, Y.; Li, W.; Wu, P.; Zhang, H.; Cai, C. *Anal. Chem.* **2013**, *85*, 2536−2542.
(14) Zhou, J.; Xu, X.; Liu, W.; Liu, X.; Nie, Z.; Qing, M.; Nie, L.; Yao, S. *Anal. Chem.* **2013**, *85*, 5746−5754.
(15) Liu, X.; Wang, F.; Aizen, R.; Yehezkeli, O.; Willner, I. *J. Am. Chem. Soc.* **2013**, *135*, 11832−11839.

(16) Shi, Y.; Huang, W. T.; Luo, H. Q.; Li, N. B. *Chem. Commun.* **2011**, *47*, 4676−4678.
(17) Feng, D.; Zhang, Y.; Feng, T.; Shi, W.; Li, X.; Ma, H. *Chem. Commun.* **2011**, *47*, 10680−10682.
(18) Cai, L.; Zhan, R.; Pu, K.-Y.; Qi, X.; Zhang, H.; Huang, W.; Liu, B. *Anal. Chem.* **2011**, *83*, 7849−7855.
(19) Kundu, A.; Layek, R. K.; Kuila, A.; Nandi, A. K. *ACS Appl. Mater. Interfaces* **2012**, *4*, 5576−5582.
(20) Mei, Q.; Jiang, C.; Guan, G.; Zhang, K.; Liu, B.; Liu, R.; Zhang, Z. *Chem. Commun.* **2012**, *48*, 7468−7470.
(21) Wang, D; Wang, L; Dong, X. Y.; Shi, Z; Jin, J. *Carbon* **2012**, *50*, 2147−2154.
(22) Wen, Y.; Xing, F.; He, S.; Song, S.; Wang, L.; Long, Y.; Li, D.; Fan, C. *Chem. Commun.* **2010**, *46*, 2596−2598.
(23) Xie, W. Y.; Huang, W. T.; Li, N. B.; Luo, H. Q. *Chem. Commun.* **2012**, *48*, 82−84.
(24) Huang, W. T.; Xie, W. Y.; Shi, Y.; Luo, J. Q.; Li, N. B. *J. Mater. Chem.* **2012**, *22*, 1477−1481.
(25) Huang, J.; Zheng, Q.; Kim, J.-K.; Li, Z. *Biosens. Bioelectron.* **2013**, *43*, 379−383.
(26) Li, X.; Wang, G.; Ding, X.; Chen, Y.; Gou, Y.; Lu, Y. *Phys. Chem. Chem. Phys.* **2013**, *15*, 12800−12804.
(27) Kong, L.; Wang, J.; Zheng, G.; Liu, J. *Chem. Commun.* **2011**, *47*, 10389−10391.
(28) Li, M.; Zhou, X.; Ding, W.; Guo, S.; Wu, N. *Biosens. Bioelectron.* **2013**, *41*, 889−893.
(29) Liu, M.; Zhao, H.; Chen, S.; Yu, H.; Zhang, Y.; Quan, X. *Biosens. Bioelectron.* **2011**, *26*, 4111−4116.
(30) Wen, Y.; Peng, C.; Li, D.; Zhuo, L.; He, S.; Wang, L.; Huang, Q.; Xu, Q. H.; Fan, C. *Chem. Commun.* **2011**, *47*, 6278−6280.
(31) Liu, M.; Zhao, H.; Chen, S.; Yu, H.; Zhang, Y.; Quan, X. *Chem. Commun.* **2011**, *47*, 7749−7751.
(32) Marcano, D. C.; Kosynkin, D. V.; Berlin, J. M.; Sinitskii, A.; Sun, Z. Z.; Slesarev, A.; Alemany, L. B.; Lu, W.; Tour, J. M. *ACS Nano* **2010**, *4*, 4806−4814.
(33) Balapanuru, J.; Yang, J. X.; Xiao, S.; Bao, Q. L.; Jahan, M.; Polavarapu, L.; Wei, J.; Xu, Q. H.; Loh, K. P. *Angew. Chem., Int. Ed.* **2010**, *49*, 6549−6553.
(34) Kudin, K. N.; Ozbas, B.; Schniepp, H. C.; Prud'homme, R. K.; Aksay, I. A.; Car, R. *Nano Lett.* **2008**, *8*, 36−41.
(35) Zhou, X. Z.; Huang, X.; Qi, X. Y.; Wu, S. X.; Xue, C.; Boey, F. Y. C.; Yan, Q. Y.; Chen, P.; Zhang, H. *J. Phys. Chem. C* **2009**, *113*, 10842−10846.
(36) Jain, P. K.; Lee, K. S.; El-Sayed, I. H.; El-Sayed, M. A. *J. Phys. Chem. B* **2006**, *110*, 7238−7248.
(37) Makarova, O. V.; Ostafin, A. E.; Miyoshi, H.; Norris, J. R.; Meisel, D. *J. Phys. Chem. B* **1999**, *103*, 9080−9084.
(38) Feng, D.; van Deventer, J. S. J. *Hydrometallurgy* **2002**, *64*, 231−246.
(39) Chen, Y. Y.; Chang, H. T.; Shiang, Y. C.; Hung, Y. L.; Chiang, C. K.; Huang, C. C. *Anal. Chem.* **2009**, *81*, 9433−9439.
(40) Lee, Y. F.; Huang, C. C. *ACS Appl. Mater. Interfaces* **2011**, *3*, 2747−2754.
(41) Zhang, Y.; Leng, Y.; Miao, L.; Xin, J.; Wu, A. *Dalton Trans.* **2013**, *42*, 5485−5490.
(42) Bryce, R. A.; Charnock, J. M.; Pattrick, R. A. D.; Lennie, A. R. *J. Phys. Chem. A* **2003**, *107*, 2516−2523.
(43) Deschenes, G.; Lastra, R.; Brown, J. R.; Jin, S.; May, O.; Ghali, E. *Miner. Eng.* **2000**, *13*, 1263−1279.
(44) Yasuda, H.; Mori, H. *Philos. Mag. A* **1996**, *73*, 567−573.
(45) Haiss, W.; Thanh, N. T. K.; Aveyard, J.; Fernig, D. G. *Anal. Chem.* **2007**, *79*, 4215−4221.
(46) Senanayake, G. *Hydrometallurgy* **2008**, *90*, 46−73.
(47) Fu, X.; Lou, T.; Chen, Z.; Lin, M.; Feng, W.; Chen, L. *ACS Appl. Mater. Interfaces* **2012**, *4*, 1080−1086.
(48) Muszynski, R.; Seger, B.; Kamat, P. V. *J. Phys. Chem. C* **2008**, *112*, 5263−5266.
(49) Xu, C.; Wang, X.; Zhu, J. *J. Phys. Chem. C* **2008**, *112*, 19842−19845.
(50) Shen, J.; Hu, Y.; Shi, M. *J. Phys. Chem. C* **2010**, *114*, 1498−1503.
(51) Praharaj, S.; Ghosh, S. K.; Nath, S.; Kundu, S.; Panigrahi, S.; Basu, S.; Pal, T. *J. Phys. Chem. B* **2005**, *109*, 13166−13174.